Journal of Cerebral Blood Flow & Metabolism (2006), 1-13

www.jcbfm.com

Novel therapeutic strategy for stroke in rats by bone marrow stromal cells and *ex vivo* HGF gene transfer with HSV-1 vector

Ming-Zhu Zhao[1,2], Naosuke Nonoguchi[1], Naokado Ikeda[1], Takuji Watanabe[1], Daisuke Furutama[3], Daisuke Miyazawa[4], Hiroshi Funakoshi[4], Yoshinaga Kajimoto[1], Toshikazu Nakamura[4], Mari Dezawa[5], Masa-Aki Shibata[6], Yoshinori Otsuki[6], Robert S Coffin[7], Wei-Dong Liu[2], Toshihiko Kuroiwa[1] and Shin-Ichi Miyatake[1]

[1]*Department of Neurosurgery, Osaka Medical College, Takatsuki, Osaka, Japan;* [2]*Department of Neurosurgery, Pu Nan Hospital, Shanghai, People's Republic of China;* [3]*First Department of Internal Medicine, Osaka Medical College, Takatsuki, Osaka, Japan;* [4]*Division of Molecular Regenerative Medicine, Osaka University Graduate School of Medicine, Suita, Osaka, Japan;* [5]*Department of Anatomy and Neurobiology, Kyoto University Graduate School of Medicine, Kyoto, Japan;* [6]*Department of Anatomy and Biology, Osaka Medical College, Takatsuki, Osaka, Japan;* [7]*Department of Molecular Pathology in Windeyer Institute of Medical Sciences of University College, London, UK*

Occlusive cerebrovascular disease leads to brain ischemia that causes neurological deficits. Here we introduce a new strategy combining mesenchymal stromal cells (MSCs) and *ex vivo* hepatocyte growth factor (HGF) gene transferring with a multimutated herpes simplex virus type-1 vector in a rat transient middle cerebral artery occlusion (MCAO) model. Gene-transferred MSCs were intracerebrally transplanted into the rats' ischemic brains at 2 h (superacute) or 24 h (acute) after MCAO. Behavioral tests showed significant improvement of neurological deficits in the HGF-transferred MSCs (MSC-HGF)-treated group compared with the phosphate-buffered saline (PBS)-treated and MSCs-only-treated group. The significant difference of infarction areas on day 3 was detected only between the MSC-HGF group and the PBS group with the superacute treatment, but was detected among each group on day 14 with both transplantations. After the superacute transplantation, we detected abundant expression of HGF protein in the ischemic brain of the MSC-HGF group compared with others on day 1 after treatment, and it was maintained for at least 2 weeks. Furthermore, we determined that the increased expression of HGF was derived from the transferred *HGF* gene in gene-modified MSCs. The percentage of apoptosis-positive cells in the ischemic boundary zone (IBZ) was significantly decreased, while that of remaining neurons in the cortex of the IBZ was significantly increased in the MSC-HGF group compared with others. The present study shows that combined therapy is more therapeutically efficient than MSC cell therapy alone, and it may extend the therapeutic time window from superacute to acute phase.
Journal of Cerebral Blood Flow & Metabolism advance online publication, 18 January 2006; doi:10.1038/sj.jcbfm.9600273

Keywords: gene transfer; hepatocyte growth factor; herpes simplex virus; intracerebral transplantation; mesenchymal stromal cell; transient cerebral ischemia

Introduction

Occlusive cerebrovascular disease often causes global ischemia of the brain and results in neuropathological changes. Several methods have been proposed to augment brain reorganization, including the stimulation of endogenous processes through pharmacologic or molecular manipulation, gene therapy, behavioral and rehabilitation strategies, and the provision of new substrates for recovery through cell therapy.

Bone marrow contains the precursors of nonhematopoietic tissues that are referred to as mesenchymal stem cells or marrow stromal cells (MSCs) (Friedenstein *et al*, 1978). Marrow stromal cells are characterized by the ability to self-renew in a number of nonhematopoietic tissues, and by their

Correspondence: Dr S-I Miyatake and Dr T Kuroiwa, Department of Neurosurgery, Graduate School of Medicine, Osaka Medical College, 2-7 Daigakumachi, Takatsuki City, Osaka 569-8686, Japan. E-mail: neu070@poh.osaka-med.ac.jp
This work was supported by Grants-in-Aid for Scientific Research (B) (14370448) and (C) (12671353), and by a Grant-in-Aid for Exploratory Research (14657350) from the Japanese Ministry of Education, Science and Culture, Japan to Shin-Ichi Miyatake, MD, PhD. Additional support was provided in the form of a grant from the Special Assistance for Promoting the Advancement of the Education & Research of the Private University, Promotion and Mutual Aid Corporation for Private Schools of Japan and the Science Research Promotion Fund to Shin-Ichi Miyatake, MD, PhD, and by the High-Tech Research Program of Osaka Medical College. This work was also supported in part by Grants-in-Aid 17790989 from the Ministry of Education, Science and Culture, Japan to Naosuke Nonoguchi, MD.
Received 22 August 2005; revised 29 November 2005; accepted 5 December 2005

multipotentiality for differentiation into various tissues, such as fibroblasts, bone, muscle, and cartilage (Caplan and Bruder, 2001; Phinney, 2002). Additionally, they share some characteristics of neurons and astrocytes when cultured *in vitro* (Kim *et al*, 2002) or after being implanted into the central nervous system *in vivo* (Chopp *et al*, 2000; Nakano *et al*, 2001; Li *et al*, 2001, 2002; Chen *et al*, 2002*a*, *b*). Marrow stromal cells can also secrete growth factors and cytokines into the soluble stromal and neurochemicals into the brain (Li *et al*, 2002; Chen *et al*, 2002*a*, *b*), cross the blood–brain barrier (BBB) and migrate throughout the brain preferentially to areas that have suffered damage (Chen *et al*, 2000; Li *et al*, 2000, 2001; Damme *et al*, 2002). Many previous researchers have reported on mesenchymal stromal cell (MSC) transplantation as a source for autoplastic therapies and improvement in functional recovery after stroke (Chen *et al*, 2000; Li *et al*, 2000, 2001, 2002; Rempe and Kent, 2002; Kurozumi *et al*, 2004).

Hepatocyte growth factor (HGF) is a disulfide-linked heterodimeric protein that was initially purified and cloned as a potent mitogen for hepatocytes and a natural ligand for the c-met proto-oncogene product (Nakamura *et al*, 1984; Matsumoto and Nakamura, 1996). Subsequently, several functions have been ascribed to HGF, including antiapoptosis, angiogenesis, motogenesis, morphogenesis, hematopoiesis, tissue regeneration in a variety of organs, and the enhancement of neurite outgrowth (Matsumoto and Nakamura, 1997; Hayashi *et al*, 2001; Sun *et al*, 2002*a*, *b*; Jin *et al*, 2003). It has also been reported that HGF administration could inhibit the BBB destruction, decrease brain edema, and provide a neuroprotective effect after brain ischemia (Miyazawa *et al*, 1998; Hayashi *et al*, 2001; Shimamura *et al*, 2004).

Recent experimental studies suggest the possibility that gene transduction into MSCs could enhance their existing therapeutic potential (Chen *et al*, 2000; Kurozumi *et al*, 2004). Here, we evaluate the efficiency and effects of gene transduction into MSCs using a replication-incompetent herpes simplex virus type-1 (HSV1764/4-/pR19) vector disabled by the deletion of three critical genes for viral replication encoding infected cell polypeptide (ICP)4, ICP34.5, and virion protein (VP16) (vmw65). This vector contains HSV latency-associated transcript (LAT) promoter and two kinds of enhancer elements: cytomegalovirus (CMV) enhancer and Woodchuck posttranscriptional regulatory elements (WPRE). The availability of this vector has already been examined in the nervous system (Coffin *et al*, 1998; Palmer *et al*, 2000; Lilley *et al*, 2001).

In the present study, we intracerebrally transplanted MSCs in which a gene of interest was transferred with this HSV-1 vector *ex vivo* into a rat transient middle cerebral artery occlusion (MCAO) model under superacute and acute therapeutic time phase, and investigated whether such combined therapy could improve the effects of ischemia.

Materials and methods

Donor Cell Preparation

Marrow stromal cells of adult Wistar rats were prepared following the method described by Azizi *et al* (1998). In brief, the marrow of rat tibias and femurs was extruded with 10 mL of alpha-MEM (Sigma Chemical Co., St Louis, MO, USA) and cultured in the same medium supplemented with 10% fetal bovine serum (FBS), 2 mmol/L L-glutamine, and antibiotic–antimycotic 1 mL/100 mL (GIBCO Invitrogen, Carlsbad, CA, USA) at 37°C, 98% humidity and 5% CO_2. After 48 h, the nonadherent cells were removed by replacing the medium, and the adherent cells were continuously subcultured as MSCs. The fifth to seventh passages were used for the following experiments.

HSV1764/-4/pR19-Hepatocyte Growth Factor Virus and Propagation

One of the authors of the current study (Coffin) constructed the prototype HSV1764/4/pR19GFP virus and has previously described this vector's characteristics (Palmer *et al*, 2000; Lilley *et al*, 2001), which are also described briefly in the Introduction. In the present study, the green fluorescent protein (*GFP*) gene was replaced with a full-length rat HGF complementary DNA (cDNA) tagged with the KT3 (SV (simian virus)40 large, T antigen) epitope (ratHGFKT3) (Sun *et al*, 2002*b*), and the authenticity of this vector (pR19ratHGFKT3WPRE) was confirmed by sequence analysis. Homologous recombination was performed in M49 cells by cotransfection of plasmid pR19ratHGFKT3WPRE DNA and HSV1764/-4/pR19GFP viral DNA. White plaques were selected and purified three times, and replication-incompetent viruses were propagated as described previously (Palmer *et al*, 2000). We ultimately obtained the HSV1764/-4/pR19-HGF virus (HSV-HGF) with a titer of 2×10^8 pfu/mL for use in the present experiments.

Ex Vivo Gene Delivery to MSCs

The cultured MSCs from the fifth to seventh passages were infected with the virus suspension by incubation for 1 h. After infection, the virus suspension was changed to normal culture medium for MSCs and continuously cultured for the subsequent 24 h before transplantation.

Our previous experiments show that the transduction efficiency of the *GFP* gene into the MSCs with our HSV-1 vector is more than 50% even with a multiplicity of infection (MOI) of 5. Here we set the MOI at 5 for the desired gene transfer to MSCs *ex vivo*.

Hepatocyte Growth Factor Detection with Enzyme-Linked Immunosorbent Assay (ELISA) *In Vitro*

We prepared 1.6×10^5 MSCs in each well of a six-well dish. The MSCs were transferred with *HGF* gene by infection with HSV-HGF at MOIs of 0, 0.1, 1, 5, and 10. At 1 h after infection, the infected MSCs were successively incubated with normal culture medium for another 24 h. The culture supernatant and cells were then individually collected through centrifugation. The HGF protein concentrations in MSC culture supernatant and in MSC extracts prepared using 50 mmol/L Tris-HCl (pH 7.4), 150 mmol/L NaCl, 1% Triton X-100, 1 mmol/L phenylmethylsulfonylfluoride (PMSF) (Wako, Osaka, Japan), 2 μg/ml antipain (Peptide Institute Inc., Osaka, Japan), 2 μg/ml leupeptin (Peptide Institute), and 2 μg/ml pepstatin (Peptide Institute) were determined by ELISA using an anti-rat HGF polyclonal antibody (Tokushu Meneki, Tokyo, Japan) as described (Sun *et al*, 2002*b*).

Transient Middle Cerebral Artery Occlusion Animal Model

Experiments were performed on 8-week-old male Wistar rats weighing 250 to 280 g. We induced transient MCAO using the previously described method of intraluminal vascular occlusion (Longa *et al*, 1988). In brief, a length (18.5 to 19.0 mm, determined according to the animal's weight) of 4-0 surgical nylon suture was gently advanced from the external carotid artery into the lumen of the internal carotid artery until it reached the proximal segment of the anterior cerebral artery. After 2 h of MCAO the animals were reanesthetized, and reperfusion was achieved by withdrawing the nylon suture.

The rats were subjected to transient MCAO for 2 h to produce a consistent and reproducible ischemic lesion in the unilateral striatum and cortex.

Intracerebral Transplantation of MSCs

At 2 or 24 h after the onset of MCAO (i.e., on reperfusion), the animals were placed in a stereotactic head holder (model 900, David Kopf Instruments, Tujunga, CA, USA) under inhalation anesthesia. MSCs were intracerebrally transplanted by inserting a 26-gauge needle with a Hamilton syringe into the right striatum (anteroposterior (AP) = 0 mm; lateral to midline (ML) = 2.0 mm; vertical to dura (DV) = 4.5 mm) from bregma, based on the atlas given by Paxinos *et al* (1985). There were 1×10^6 cells in total 10-μl fluid volumes that transplanted into each animal over a 10-min period. No immunosuppressive drugs were used in any animal.

Experimental Groups

In this study, there were seven experimental groups: groups 1 and 5 were treated with phosphate-buffered saline (PBS); groups 2 and 6 were treated with untreated MSCs only; group 3 was treated with the GFP-transferred MSCs (MSC-GFP); and groups 4 and 7 were treated with *HGF* gene-transferred MSCs (MSC-HGF).

Groups 1 to 4 were treated 2 h after MCAO (superacute phase) and groups 5 to 7 were treated 24 h after MCAO (acute phase).

Behavioral Testing

The rats of groups 1 to 4 ($n = 6$) were subjected to a modified neurological severity score (mNSS) test (Schallert *et al*, 1997) to evaluate neurological function before MCAO, at 2 h after MCAO, and at 1, 4, 7, 14, 21, 28, and 35 days after MCAO. The rats of groups 5 to 7 ($n = 6$) were subjected to mNSS before MCAO and at 0, 1, 4, 7, and 14 days after MCAO. These tests are battery of motor, sensory, reflex, and balance tests, which are similar to the contralateral neglect tests in humans. The higher the score, the more severe the neurological deficit (Chen *et al*, 2001).

Infarction Volume

We stained the brains of groups 1, 2, and 4 ($n = 6$) and groups 5 to 7 ($n = 5$) with 2,3,5-triphenyltetrazolium chloride (TTC) (Wako Pure Chemical Industries, Osaka, Japan) to detect the infarction volume of each group at 3 and 14 days after treatment. Briefly, the rats' brains were removed and cut into seven equally spaced (2 mm) coronal sections. These sections were immersed in a 2% solution of TTC at 37°C for 20 mins to reveal the infarcted areas. This procedure is known to reliably mark ischemic damage even at 14 days after MCAO (Bederson *et al*, 1986; Kurozumi *et al*, 2005).

The disposition of the ischemic area was evaluated by calculating the hemispheric lesion area using imaging software (Scion Image, version Beta 4.0.2; Scion Corp., Frederick, MD, USA). To avoid overestimation of the infarct volume, the corrected infarct volume (CIV) was calculated as $CIV = [LT-(RT-RI)] \times d$, where LT is the area of the left hemisphere, RT is the area of the right hemisphere, RI is the infarcted area, and d is the slice thickness (2 mm) (Raymond *et al*, 1990). Relative infarct volumes are expressed as a percentage of contralateral hemispheric volume.

Terminal Deoxynucleotidyltransferase (dUTP) Nick End-Labeling (TUNEL) Staining and Immunohistochemical Assessment

Sample Preparation: At different time points, rats of groups 1, 2, and 4 were reanesthetized and transcardially perfused with saline, followed by 4% paraformaldehyde in PBS. The brain tissues were cut into seven equally spaced coronal blocks. The tissues were processed and 10-μm cryosections were cut.

Immunohistochemical Staining: We can detect three kinds of HGF in this study: the endogenous HGF secreted by the rat ischemic brain tissue after stoke (en-HGF), the exogenous HGF secreted by the transplanted MSCs (ex-HGF-1), and the exogenous HGF delivered from the

HSV-HGF (ex-HGF-2). For the immunohistochemical staining of HGF, the whole rats' brain sections of groups 1, 2, and 4 were prepared on days 2 and 14 after treatment. Rabbit anti-rat HGF primary antibody (prepared by some of the authors of this article, and belonging to the Division of Molecular Regenerative Medicine, Osaka University Graduate School of Medicine, Japan) was used to detect the three kinds of HGF (mixed); a KT3 primary monoclonal antibody (1:1000) (Covance Research Products, Berkeley, CA, USA) was used to detect the ex-HGF-2; a biotinylated universal secondary antibody (VECSTAIN Elite ABC Kit, PK-6200, Vector Laboratories, Burlingame, CA, USA) and a goat anti-rabbit IgG affinity-purified rhodamine-conjugated secondary antibody (1:200) (Chemicon International, Temecula, CA, USA) were also used here. Reaction products were visualized with the VECSTAIN Elite ABC Kit (PK-6200) and a DAB Substrate Kit (Vector Laboratories, Burlingame, CA, USA). To detect the donor MSCs, bisbenzimide (Hoechst 33258; Polysciences, Eppelheim, Germany) was used to fluorescently label cell nuclei *in vitro*. Some sections were counterstained with hematoxylin and observed under a normal light microscope (VB-S20 Multiviewer System, Keyence, Osaka, Japan and Microphot-FXA, Nikon Corp., Tokyo, Japan), and some were directly observed by a fluorescence microscope (BX-50-34-FLAD1, Olympus). The donor MSCs could be detected under ultraviolet (UV) light with blue fluorescence as marked by Hoechst 33258.

To visualize the remaining neurons in the cortex of the ischemic boundary zone (IBZ) of groups 1, 2, and 4 ($n = 3$), 7 days after treatment, microtubule-associated protein 2 (MAP-2) was used as the first antibody (1:500) (Chemicon International Inc., CA, USA). Negative control slides for each animal received identical preparation for immunohistochemical staining, except that primary antibodies were omitted.

Terminal Deoxynucleotidyltransferase Nick End-Labeling Staining: At 7 days after treatment, coronal cryosections (10-μm thick) of each rat of groups 1, 2, and 4 ($n = 3$) were stained by the TUNEL method for *in situ* apoptosis detection (ApopTag kit, Chemicon International, USA). Specifically, after postfix slides were incubated in a mixture containing terminal deoxynucleotidyl transferase and anti-digoxigenin-rhodamine (Red). Then, they were counterstained with bisbenzimide (Hoechst 33258), which stains blue for each nucleus. The total numbers of TUNEL-positive cells and Hoechst counter-staining positive cells were individually counted in 2 slides from each brain, with each slide containing five random fields from the IBZ, under an $\times 20$ objective of the fluorescence microscope system (BX-50-34-FLAD1, Olympus), using a 3-CCD color video camera (Keyence VB-7010, Keyence, Osaka, Japan).

Statistical Analysis

Data are presented as means $\pm$ standard deviations (s.d.). Data from the behavior test (mNSS) were evaluated with repeated-measures analysis of variance (ANOVA), with subsequent Fisher's protected least significant difference (PLSD) test. StatView 5.0 software (SAS Institute, Cary, NC, USA) performing the Student's *t*-test was used to test the CIV data and the difference in means of percentage of the apoptosis-positive cells and the remaining neurons. A difference with a probability value of $P \leq 0.05$ was considered to be statistically significant.

Results

Quantification of Hepatocyte Growth Factor Analysis with Enzyme-Linked Immunosorbent Assay *In Vitro*

As a result, the HGF concentration was approximately 15 times higher in the culture supernatant than in the cell extract at the same MOI, and its increase was correlated with an increase in MOI. Although normal MSCs can produce HGF protein at 0.4 ng/1.6×10^5 cells/24 h, after the MSCs were infected with HSV-HGF at an MOI of 5, they were found to produce HGF protein at 2.4 ng/1.6×10^5 cells/24 h (Figure 1).

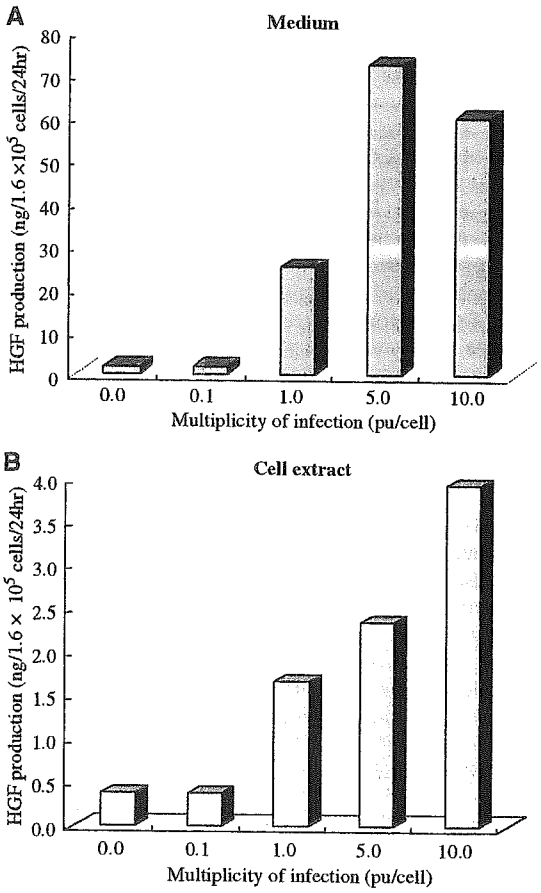

Figure 1 Enzyme-linked immunosorbent assay to determine HGF concentration *in vitro*. Hepatocyte growth factor concentrations were detected in MSC culture supernatant (**A**) and in MSC cell extract. (**B**) After 24 h, 1.6×10^5 MSCs were transfected with HSV-HGF at MOIs of 0, 0.1, 1, 5, and 10.

Neurological Outcome

No significant difference in neurological function was detected among all the groups just before cell transplantation. Significant differences of functional recovery were found in group 1 individually compared with group 2 (days 14 to 35, $P<0.05$), with group 3 (days 21 to 35, $P<0.05$), and with group 4 (days 4 and 7, $P<0.05$; days 14 to 35, $P<0.01$) during the observation periods after the superacute transplantation (Figure 2A), and in group 5 individually compared with group 6 (day 14, $P<0.05$), with group 7 (day 7, $P<0.01$ and day 14, $P<0.01$) after the acute transplantation (Figure 2B). Interestingly, we observed significant differences of functional recovery on day 14 among all the superacute treated groups including the MSC-GFP group, which served as a control for *ex vivo* nontherapeutic gene transduction ($P<0.05$). Exceptionally, there was no significant difference only between the MSC-only and the MSC-GFP groups at that time point (Figure 2A). We also found significant neurological recovery on day 14 in the combined therapy group treated even in the acute phase, compared with the MSC-only group treated in the superacute phase (Figure 2C). Also, significant difference of functional recovery on day 14 was found among the groups treated in the acute phase (Figure 2B).

Quantitative Analysis of Infarct Volume

We compared the infarction areas in coronal sections of groups 1, 2, and 4 on day 3 (Figure 3A) and day 14 (Figure 3B), and compared those of groups 5 to 7 on the same time points by TTC staining, and expressed lesion volume as a percentage of contralateral hemispheric volume. At 3 days after treatment, significant difference of %CIV was only detected in the MSC-HGF group compared with the PBS group ($34.52\% \pm 3.44\%$ versus $41.83\% \pm 6.25\%$, $P<0.05$), both of which were treated in the superacute phase (Figure 3C). However, on day 3 there was no significant difference of %CIV among any group that was treated in the acute phase (Figure 3C), while on day 14 there were significant reductions of %CIV in the rats of the MSC-HGF group compared with not only the PBS group but also the MSC-only group treated in the both therapeutic phases (Figure 3D). Also on day 14, the rats treated with MSC-only showed significant reduction in %CIV compared with the PBS group that was treated in the superacute phase (Figure 3D).

Hepatocyte Growth Factor and herpes simplex virus type Gene-Transferred Hepatocyte Growth Factor Detection *In Vivo*

The macrographs presented in Figure 4 showed that mixed HGF protein was diffusely overexpressed in almost the whole ipsilateral brain in the MSC-HGF group compared with other groups, not only on day 2 (column A) but throughout at least the first 2 weeks (column C) after treatment. The microphotographs presented in column B of Figure 4 showed that high HGF expression in the MSC-HGF group could be detected in both the ipsilateral cortex and the ipsilateral basal ganglia at 2 days after treatment. Nevertheless, almost no HGF expression could be detected on the contralateral hemisphere in any treatment group (Figure 4).

Fluorescent staining of groups 1, 2, and 4 on day 14 (Figure 5, column C) also showed higher mixed HGF expression in the MSC-HGF group than that of the other groups. Also, we could detect donor MSCs with blue fluorescence expression by direct observation under UV light (Figure 5, column B). We could identify the HGF expression with red fluorescence in both the transplanted cells and the intercellular space in the transplantation area.

Furthermore, we detected ex-HGF-2 expression, which was transferred from HSV-HGF by anti-KT3 staining (Figures 6D to 6F) of the implantation area. As a result, we had identified ex-HGF-2 expression both in the *HGF* gene-transferred MSCs (arrows in Figure 6G) and in the intercellular space of the transplantation area (arrowheads in Figure 6G) only in the MSC-HGF group (Figure 6F) even 14 days after transplantation. Additionally, we confirmed that MSC itself can also secrete HGF *in vivo* (Figure 6B).

Antiapoptosis

Using TUNEL staining (Figure 7, columns B and C), apoptotic cells with red fluorescence were counted in the IBZ 7 days after treatment, while cells were counted in the same area with blue fluorescence by Hoechst 33258 nuclei marking. In this area we could not detect transferred MSCs; therefore, counterstained cells seemed to be host-derived. The percentage of apoptotic host cells was significantly decreased in the MSC-HGF group ($4.92\% \pm 2.15\%$) compared with the PBS group ($22.12\% \pm 4.28\%$, $P<0.01$) and MSC-only group ($10.73\% \pm 5.64\%$, $P<0.01$). However, there was also significant decrease of apoptotic cells between the MSC-only group ($10.73\% \pm 5.64\%$) and the PBS group ($22.12\% \pm 4.28\%$, $P<0.01$) (Figure 7C).

Neuroprotection

Immunohistochemical staining revealed the remaining neurons of the host with MAP-2 neuronal marker 7 days after treatment (Figure 8A). The percentage of remaining neurons in the cortex of IBZ significantly increased in the MSC-HGF group ($20.73\% \pm 2.38\%$) compared with the PBS group ($7.75\% \pm 1.58\%$, $P<0.01$) and the MSC-only group ($12.13\% \pm 3.05\%$, $P<0.01$). Also, the significant

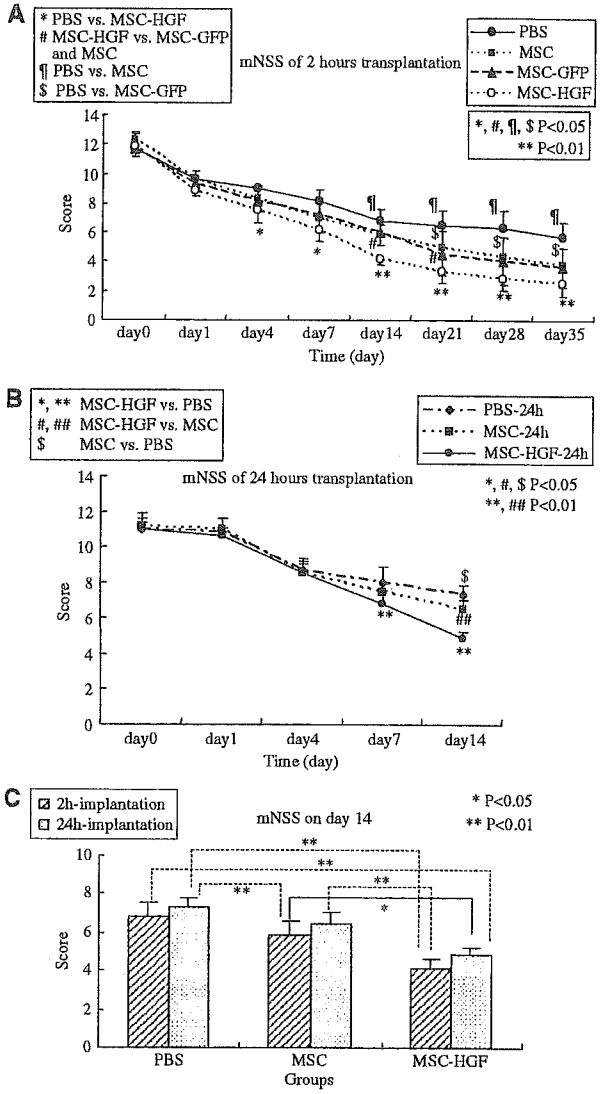

Figure 2 Behavioral functional test (mNSS) before and after MCAO. Groups 1 and 5: treated with PBS; groups 2 and 6: treated with MSC-only; group 3: treated with MSC-GFP; groups 4 and 7: treated with MSC-HGF ($n = 6$ per group). The rats of groups 2 to 7 received 1.0×10^6 cells via intracerebral transplantion in 10 μl PBS. (**A**) Groups 2 to 4 received transplantation 2 h after MCAO (superacute phase); (**B**) groups 4 to 7 received transplantation 24 h after MCAO (acute phase). (**C**) Lists the mNSS on day 14 of groups 1, 2, 4, 5, 6, and 7, showing that the significant neurological recovery among 6 groups while under the comparing condition is only the different therapeutic time phase. Significant functional recovery was detected in the MSC-HGF group compared with the other groups. Data are presented as means $\pm$ s.d.

increase of remaining neurons was found in the MSC-only group (12.13% $\pm$ 3.05%), in comparison with the PBS group (7.75% $\pm$ 1.58%, $P < 0.01$) (Figure 8B).

Discussion

Brain ischemia initiates a cascade of events that produces neuronal death and leads to neurological deficits. To prevent brain injury after ischemia, some studies have focused on cell therapies by using embryonic stem cell. But ethical and logistical problems make it unlikely that such therapy could serve as a source of material for therapeutic transplants. Recently, MSC transplantation was reported as a source of autoplastic therapies which not only improve functional recovery after stroke but also have a low risk of tumorigenesis and do not provoke immune reactions (McIntosh and Bartholomew, 2000; Li *et al*, 2002). In the present study, rats of the MSC-only and MSC-HGF groups also showed more significant neurological functional recovery than those of the PBS group.

It is well known that the efficiency of gene transduction to such MSC populations is low, even with virus vectors such as an adenovirus (Ad) (Conget and Minguell, 2000). To date, Kurozumi *et al* (2004) have reported the relatively high efficiency of gene transduction using fiber mutant Ad vector, but the peak level of expression was transient because the Ad vector would not integrate the gene of interest into the genome of the host cells. Lentivirus could express a high efficiency of gene transduction into MSC, but its biosafety remains uncertain because of its origin, the human immunodeficiency virus (Trono, 2000). Retroviruses, which have the ability to integrate the gene of interest into the chromosomes of the host cells, also show a relatively high efficiency of gene transduction to MSC. However, a note of warning was stressed against the potential rise of a neoplasm with a retrovirus-based vector (Pages and Bru, 2004).

In the present study, by the *in vitro* HGF ELISA data and histological detection, we showed that our HSV-1 vector had successfully transferred the gene of interest to the MSC population with high efficiency *in vitro*, and gene-transferred MSCs had successfully functioned *in vivo* to express and maintain a high level of the gene of interest. We confirmed that the increased HGF expression on day 14 was primarily due to the ex-HGF-2 expression that was proven by anti-KT3 staining, as the HSV-1 vector-transferred HGF cDNA was tagged with KT3 epitope. Also, such ex-HGF-2 protein was produced within the *HGF* gene-transferred MSCs and secreted in the intercellular space diffusely in the combined therapy group.

Furthermore, there were no significant differences in functional recovery between the MSC-only group and the MSC-GFP group during the whole detection time course. Also, no obvious difference of apoptosis and the dividing ability was observed between naive MSCs and the *HGF* gene-transferred MSCs in the current study in the first 2 weeks after transplantation (data not shown). It may indicate that gene transfer with HSV-1 vector *ex vivo* would

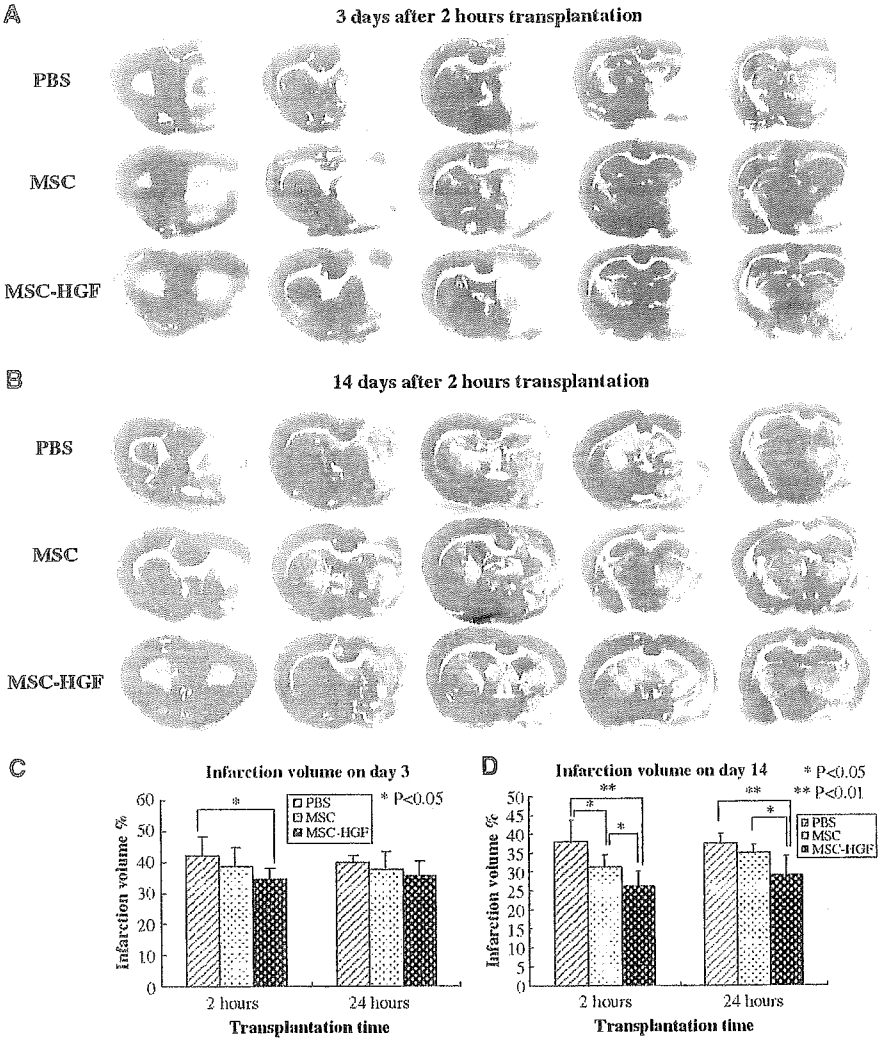

Figure 3 Infarction volume detected by TTC staining. **(A, B)** Reduction of infarction areas on days 3 and 14 of groups 1, 2, and 4, which received transplantation 2 h after MCAO occurred: coronal sections stained with TTC. The red region shows intact area; white region shows infarction area. **(C, D)** Individually presents the quantification of % CIV in the hemispheric lesion area on days 3 and 14, while being treated at 2 and 24 h after ischemia occurred. Data are presented as means $\pm$ s.d. ($P < 0.05$; < 0.01). $n = 6$ for groups 1, 2, 4, and $n = 5$ for groups 5 to 7 at each time point.

not influence the survival and dividing abilities and the therapeutic efficiency of MSCs after transplantation.

So far, to reduce the disability resulting from stroke, some studies have focused on the development of neuroprotective agents such as brain-derived neurotrophic factor, the fibroblast growth factor that effectively prevents delayed neuronal death after transient brain ischemia (Kurozumi *et al*, 2004; Watanabe *et al*, 2004). Recently, overexpression of HGF that can improve the neurological sequalae by neuroprotection, reduce the infarct volume, and the likelihood of brain edema after stroke was reported (Miyazawa *et al*, 1998; Tsuzuki *et al*, 2000; Hayashi *et al*, 2001; Shimamura *et al*, 2004). It suggested that HGF should be one of the most potent growth factors for treating brain ischemia.

To detect the therapeutic efficiency of combined therapy, we tried to treat brain ischemia in the superacute and acute therapeutic phases. Both of them showed significant improvement of neurological deficits compared with MSC-only cell therapy. We got the same result as that Shimamura *et al* (2004) had reported, that HGF had the therapeutic efficiency of reducing the infarction volume after transient MCAO. We also found on day 14 that the MSC-only treated group could significantly reduce the infarction volume under the superacute treatment compared with the PBS-treated group, but not

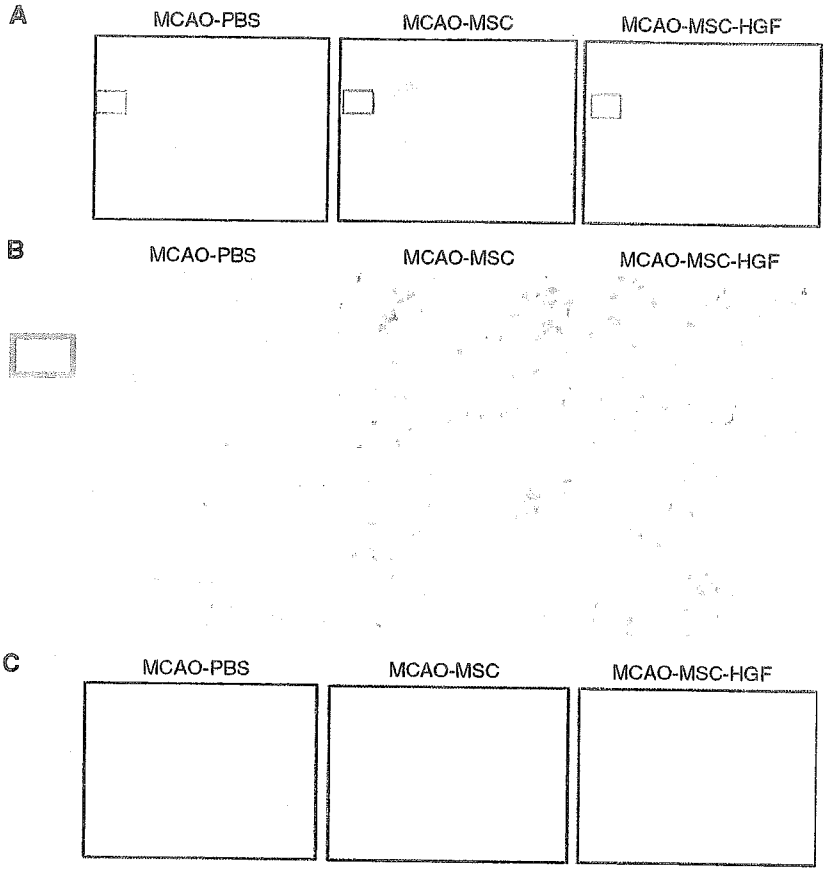

Figure 4 Immunohistochemistry for HGF expression *in vivo*. Mixed HGF expression (brown color) in the ischemic brains of groups 1, 2, and 4 detected by immunohistochemistry on days 2 (row A) and 14 (row C). Scale bar: 1.0 mm. The upper and lower rows identified in B (original magnification, × 400) show the cortex and basal ganglia, respectively, of the images shown in row A.

under the acute treatment. This was the same as the Chopp's group had reported, that transplanted MSCs to the transient MCAO model 24 h after ischemia occurred had improved neurological function recovery, but not significantly decreased infarction area (Chen *et al*, 2000, 2001; Li *et al*, 2000, 2001), while our data of the superacute treatment showed the contrast result. We thought that it might have been caused by the different therapeutic time window. Furthermore, we found significant neurological recovery of the rats treated with combined therapy on day 14, 24 h after MCAO occurred (acuter phase), than the rats of the MSC-only group treated even 2 h after MCAO occurred (superacute phase). It indicates that our combined therapeutic method may extend the therapeutic time window for treating brain ischemia at least until 24 h after the onset of MCAO, while compared with the MSC-only cell therapy. To treat transient ischemia, both the combined therapeutic method and superacute therapeutic time window might be important.

Mesenchymal stromal cell-only therapy also showed significant improvement of functional outcome and decrease of infarction volume when cells were administered 2 h after stroke. A more likely mediator of short-term benefit may reflect increased production of growth factors, including neurotrophins adjusted to the needs of the compromised tissue with an array of reducing host cells' apoptosis in the IBZ, including neurons, and promoting functional recovery of the remaining neurons (David and Thomas, 2002; Chopp and Li, 2002). After stroke, cerebral tissue reverts to an earlier stage of development and thus becomes highly responsive to stimulation by cytokines, trophins, and growth factors from the invading MSCs (Chopp and Li, 2002). The MSCs may simply provide the resources required by the ontogenous cerebral tissue to stimulate cerebral remodeling.

In the present study, the combined therapy group showed more therapeutic benefit than the MSC-only cell therapy. Hepatocyte growth factor gene-modified MSCs may also behave as small molecular factories, secrete an array of cytokines and trophic factors over an extended period and not in a single bolus dose, directly involved in promoting plasticity of the ischemic damaged neurons or in stimulating

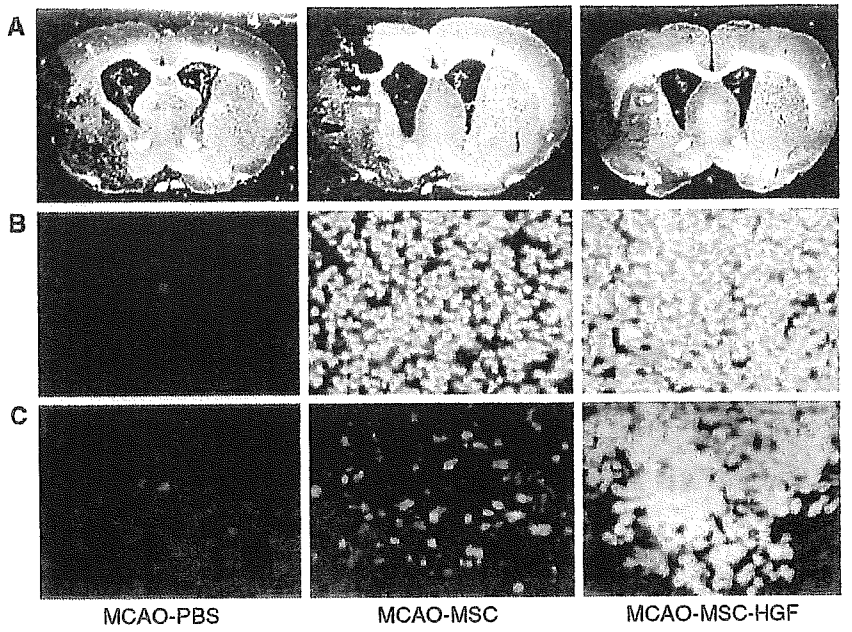

Figure 5 Expression of HGF and identification of transplanted MSCs. Photographs in row C show mixed HGF expression in the ipsilateral brain of groups 1, 2, and 4 with red fluorescence, and photographs in row B show transplanted donor MSCs of groups 2 and 4 with blue fluorescence, at 2 weeks after treatment. The microphotographs shown in rows B and C have the same size and higher power magnification than the blue squares in row A. Original magnification, × 200.

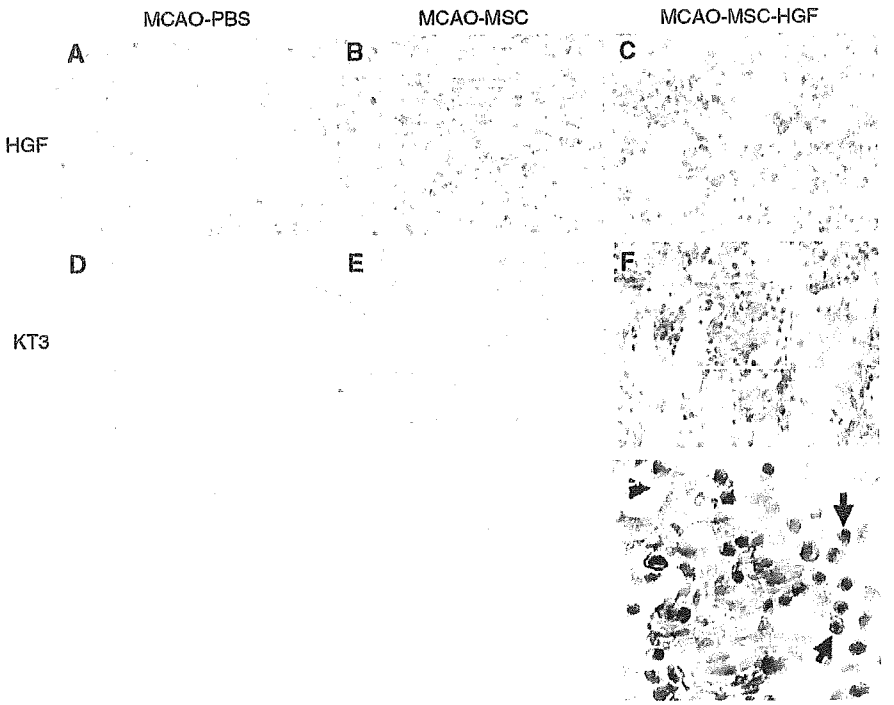

Figure 6 Immunohistochemistry for HSV-1 vector-transferred exogenous HGF and mixed HGF expression. The upper column (**A–C**) shows mixed HGF expression in groups 1, 2, and 4 with anti-rat HGF immunostaining, and the lower column (**D–F**) shows ex-HGF-2 expression with anti-ratHGFKT3 immunostaining at 2 weeks after treatment. Original magnification, × 200. (**G**) is the enlarged white square in (**F**), arrows mark HGF expression in the transplanted MSCs and an arrowhead marks HGF expression in the intracellular space.

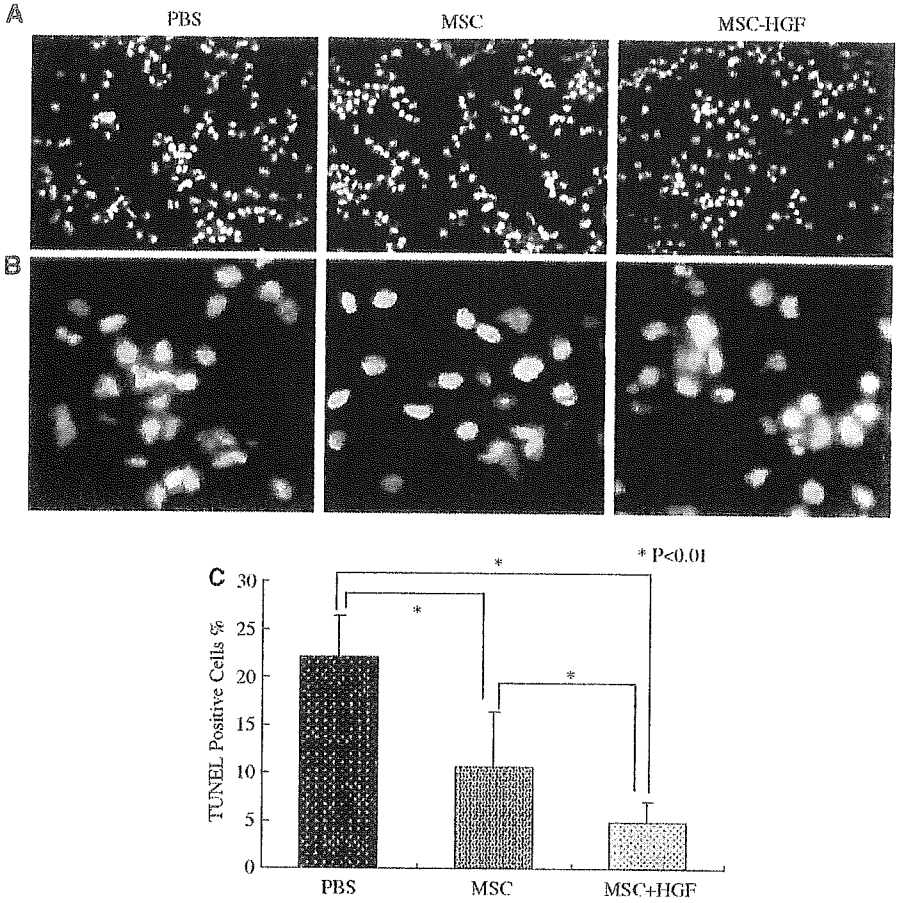

Figure 7 Apoptotic cells in the IBZ with TUNEL staining. **(A)** Column, fewer TUNEL-positive cells were detected in rats treated with MSC-HGF than others treated either with PBS or MSC-only (Rhodamine, red, TUNEL positive; Hoechst, blue, nuclear; original magnification with × 40 object). **(B)** Column, 4 times enlarged magnification of × 40 object. **(C)** The percentage of TUNEL-positive cells in the IBZ was significantly reduced in the MSC-HGF group compared with the other groups 7 days after treatment.

glial cells to secrete neurophins. Marrow stromal cells secrete many cytokines known to play a role in hematopoiesis (Dormady *et al*, 2001), and also supply autocrine, paracrine, and juxtacrine factors that influence the cells of the marrow microenvironment themselves (Haynesworth *et al*, 1996). The interaction of MSCs with the host brain may lead MSCs and parenchymal cells also to produce abundant trophic factors, which may contribute to recovery of function lost as a result of a lesion too (Williams *et al*, 1986).We speculate that *HGF* gene-modified MSCs also had carried out such ways not only to produce extended and abundant exogenous HGF, but also a variety of other cytokines and trophic factors, and interact with each other in an anatomically distributed, tissue-sensitive, and temporally ongoing way.

Other functions of HGF include reducing the BBB destruction without exacerbating cerebral edema, decreasing intracranial pressure, inducing angiogenesis, and interacting with other kinds of neurotrophic factors; cytokines that are secreted by MSCs themselves may also take part in improving the neurological recovery after stroke. We also speculate that the various cytokines secreted from MSCs or MSC-HGF activate the proliferation and differentiation of endogenous neural stem and progenitor cells in the subventricular zone, such as Chopp and Li (2002) had reported. Also, transplanted MSCs themselves might differentiate into some kinds of central never system cells (Woodbury *et al*, 2000). Actually, we also found some MSCs expressing glial phenotype 4 weeks after transplantation only in the combined therapy group (data not shown), which might suggest that *HGF* gene transduction could influence transplanted MSC differentiation. But tissue regeneration might be another part of the mechanisms that induced recovery after stroke mainly occurs in the chronic therapeutic time course.

Anyhow, our MSC-HGF combined therapy enhanced the therapeutic efficiency than the MSC-only

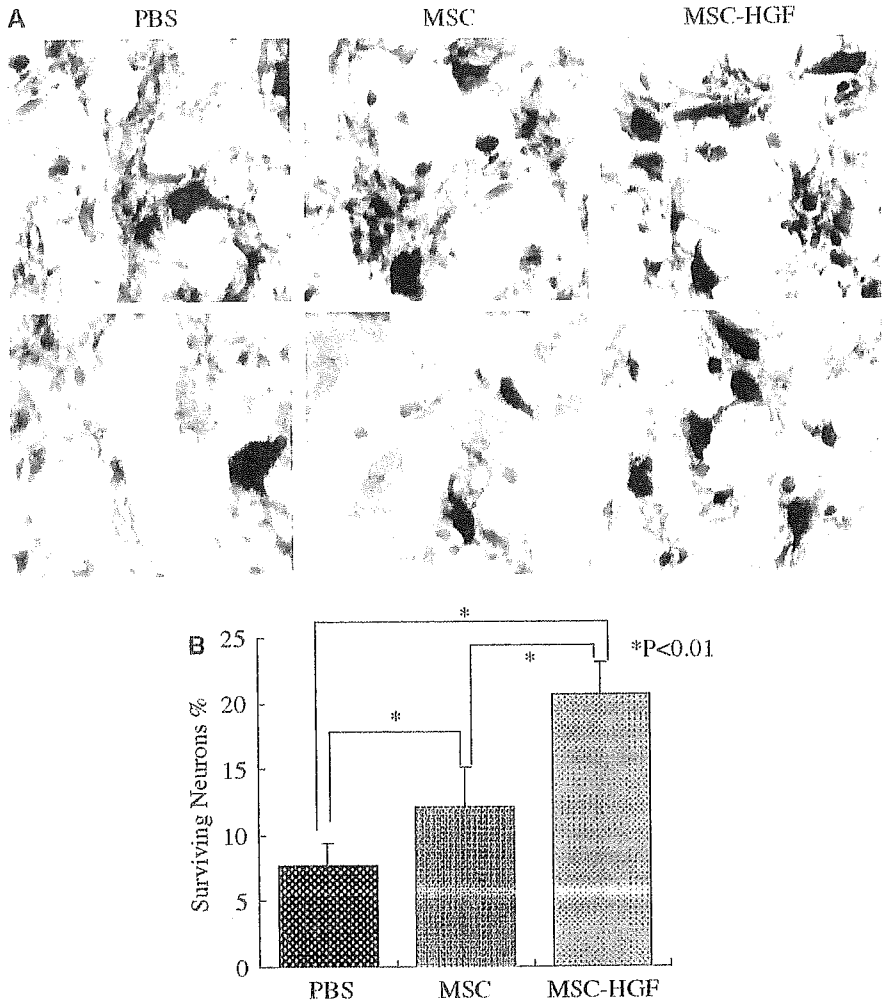

Figure 8 Remaining neurons in the cortex of IBZ with MAP-2 immunostaining. **(A)** Column, more neurons could be detected in rats treated with MSC-HGF than others treated either with PBS or MSC-only (MAP-2, dark brown, neurons; hematoxylin, blue, nuclear; original magnification, × 600). **(B)** The percentage of neurons in the cortex of IBZ was significantly increased in the MSC-HGF group compared with the other groups 7 days after treatment.

cell therapy for stroke in rats treated in both the superacute and acute phases. The target gene was successfully transferred to MSCs with the HSV-1 virus vector *in vitro*, and later the gene-modified MSCs served as both a therapeutic material and a vector platform that continuously carried the target gene into the brain and functioned *in vivo*. This method might be safer than direct gene transfer with viral vectors for *in vivo* treatments, more therapeutically efficient than MSC-only cell therapy, extend the therapeutic time window from superacute to at least 24 h after ischemia happened, and also could be used as a post-treatment method for stroke. Although the best therapeutic time schedule, the administration route of MSCs and best cytokine gene (or cocktail of the genes) should be explored for better clinical application. It may require a broad array of treatments to prevent neurological disorders in brain ischemia, which may offer a promise for human clinical treatment in future.

References

Azizi SA, Stokes D, Augelli BJ, DiGirolamo C, Prockop DJ (1998) Engraftment and migration of human bone marrow stromal cells implanted in the brains of albino rats—similarities to astrocyte grafts. *Proc Natl Acad Sci USA* 95:3908–13

Bederson JB, Pitts LH, Germano SM, Nishimura MC, Davis RL, Bartkowski HM (1986) Evaluation of 2,3,5-triphenyltetrazolium chloride as a stain for detection and quantification of experimental cerebral infarction in rats. *Stroke* 17:1304–8

Caplan AI, Bruder SP (2001) Mesenchymal stem cells: building blocks for molecular medicine in the 21st century. *Trends Mol Med* 7:259–64

Chen J, Li Y, Chopp M (2000) Intracerebral transplantation of bone marrow with BDNF after MCAO in rat. *Neuropharmacology* 39:711–6

Chen JL, Li Y, Wang L, Zhang ZG, Lu DY, Lu M *et al* (2001) Therapeutic benefit of intravenous administration of bone marrow stromal cells after cerebral ischemia in rats. *Stroke* 32:1005–11

Chen X, Katakowski M, Li Y, Lu D, Wang L, Zhang L *et al* (2002*a*) Human bone marrow stromal cell cultures conditioned by traumatic brain tissue extracts: growth factor production. *J Neurosci Res* 69:687–91

Chen X, Li Y, Wang L, Katakowski M, Zhang L, Chen J *et al* (2002*b*) Ischemic rat brain extracts induce human marrow stromal cell growth factor production. *Neuropathology* 22:275–9

Chopp M, Li Y (2002) Treatment of neural injury with marrow stromal cells. *Lancet Neurol* 1:92–100

Chopp M, Zhang XH, Li Y, Wang L, Chen J, Lu D *et al* (2000) Spinal cord injury in rat: treatment with bone marrow stromal cell transplantation. *Neuroreport* 11:3001–5

Coffin RS, Thomas SK, Thomas DP, Latchman DS (1998) The herpes simplex virus 2 kb latency associated transcript (LAT) leader sequence allows efficient expression of downstream proteins which is enhanced in neuronal cells: possible function of LAT ORFs. *J Virol* 79:3019–26

Conget PA, Minguell JJ (2000) Adenoviral-mediated gene transfer into *ex vivo* expanded human bone marrow mesenchymal progenitor cells. *Exp Hematol* 28:382–90

Damme AV, Driessche TV, Collen D, Chuah MKL (2002) Bone marrow stromal cells as targets for gene therapy. *Curr Gene Ther* 2:195–209

David AR, Thomas AK (2002) Using bone marrow stromal cells for treatment of stroke. *Neurology* 59:486–7

Dormady SP, Bashayan O, Dougherty R, Zhang XM, Basch RS (2001) Immortalized multipotential mesenchymal cells and the hematopoietic microenvironment. *J Hematother Stem Cell Res* 10:125–40

Friedenstein AJ, Ivanov-Smolenski AA, Chajlakjan RK, Gorskays UF, Kuralesova AI, Latzinik NW *et al* (1978) Origin of bone marrow stromal mechanocytes in radiochimeras and heterotopic transplants. *Exp Hematol* 6:440–4

Hayashi K, Morishita R, Nakagami H, Yoshimura S, Hara A, Matsumoto K *et al* (2001) Gene therapy for preventing neuronal death using hepatocyte growth factor: *in vivo* gene transfer of HGF to subarachnoid space prevents delayed neuronal death in gerbil hippocampal CA1 neurons. *Gene Therapy* 8:1167–73

Haynesworth SE, Baber MA, Caplan AI (1996) Cytokine expression by human marrow-derived mesenchymal progenitor cells *in vitro*: effects of dexamethasone and IL-1 alpha. *J Cell Physiol* 166:585–92

Jin H, Yang R, Li W, Ogasawara AK, Schwall R, Eberhard DA *et al* (2003) Early treatment with hepatocyte growth factor improves cardiac function in experimental heart failure induced by myocardial infarction. *J Pharmacol Exp Ther* 304:654–60

Kim BJ, Seo JH, Bubien JK, Oh YS (2002) Differentiation of adult bone marrow stem cells into neuroprogenitor cells *in vitro*. *Neuroreport* 13:1185–8

Kurozumi K, Nakamura K, Tamiya T, Kawano Y, Ishii K, Kobune M *et al* (2005) Mesenchymal stem cells that produce neurotrophic factors reduce ischemic damage in the rat middle cerebral artery occlusion model. *Mol Ther* 11:96–104

Kurozumi K, Nakamura K, Tamiya T, Kawano Y, Kobune M, Hirai S *et al* (2004) BDNF gene-modified mesenchymal stem cells promote functional recovery and reduce infarct size in the rat middle cerebral artery occlusion model. *Mol Ther* 9:189–97

Li Y, Chen J, Chen XG, Wang L, Gautam SC, Xu YX *et al* (2002) Human marrow stromal cell therapy for stroke in rat: neurotrophins and functional recovery. *Neurology* 59:514–23

Li Y, Chen J, Wang L, Lu M, Chopp M (2001) Treatment of stoke in rat with intracarotid administration of marrow stromal cells. *Neurology* 56:1666–72

Li Y, Chopp M, Chen J, Wang L, Gautam SC, Xu YX *et al* (2000) Intrastriatal transplantation of bone marrow nonhematopoietic cells improves functional recovery after stroke in adult mice. *J Cerebr Blood Flow Metab* 20:1311–9

Lilley CE, Groutsi F, Han Z, Palmer JA, Anderson PN, Latchman DS *et al* (2001) Multiple immediate-early gene-deficient herpes simplex virus vectors allowing efficient gene delivery to neurons in culture and widespread gene delivery to the central nervous system *in vivo*. *J Virol* 75:4343–56

Longa EZ, Weinstein PR, Carlson S, Cummins R (1988) Reversible middle cerebral artery occlusion without craniectomy in rats. *Stroke* 20:84–91

Matsumoto K, Nakamura T (1996) Emerging multipotent aspects of hepatocyte growth factor. *J Biochem (Tokyo)* 119:591–600

Matsumoto K, Nakamura T (1997) Hepatocyte growth factor (HGF) as a tissue organizer for organogenesis and regeneration. *Biochem Biophys Res Commun* 239: 639–44

McIntosh K, Bartholomew A (2000) Stromal cell modulation of the immune system. *Graft* 3:324–8

Miyazawa T, Matsumoto K, Ohmichi H, Katoh H, Yamashima T, Nakamura T (1998) Protection of hippocampal neurons from ischemia-induced delayed neuronal death by hepatocyte growth factor: a novel neurotrophic factor. *J Cereb Blood Flow Metab* 18:345–8

Nakamura T, Nawa K, Ichihara A (1984) Partial purification and characterization of hepatocyte growth factor from serum of hepatectomized rats. *Biochem Biophys Res Commun* 122:1450–9

Nakano K, Migita M, Mochizuki H, Shimada T (2001) Differentiation of transplanted bone marrow cells in the adult mouse brain. *Transplantation* 71:1735–40

Pages JC, Bru T (2004) Toolbox for retrovectorologists. *J Gene Med* 6(Suppl 1):S67–82

Palmer JA, Branston RH, Lilley CE, Robinson MJ, Groutsi F, Smith J *et al* (2000) Development and optimization of herpes simplex virus vectors for multiple long-term gene delivery to the peripheral nervous system. *J Virol* 74:5604–18

Paxinos G, Watson C, Pennisi M, Topple A (1985) Bregma, lambda and the interaural midpoint in stereotaxic surgery with rats of different sex, strain and weight. *J Neurosci Methods* 13:139–43

Phinney DG (2002) Building a consensus regarding the nature and origin of mesenchymal stem cells. *J Cell Biochem* 38:7–12

Raymond AS, Matthew TM, George TW, Robert AS, Charisse D, Frank RS (1990) A semiautomated method for measuring brain infarct volume. *J Cerebr Blood Flow Metab* 10:290–3

Rempe DA, Kent TA (2002) Using bone marrow stromal cells for treatment of stroke. *Neurology* 59:486–7

Schallert T, Kozlowski DA, Humm JL, Cocke RR (1997) Use-dependent structural events in recovery of function. *Adv Neurol* 73:229–38

Shimamura M, Sato N, Oshima K, Aoki M, Kurinami H, Waguri S *et al* (2004) Novel therapeutic strategy to treat brain ischemia: overexpression of hepatocyte growth factor gene reduced ischemic injury without cerebral edema in rat model. *J Circ* 109:424–31

Sun W, Funakoshi H, Nakamura T (2002*a*) Localization and functional role of hepatocyte growth factor (HGF) and its receptor c-met in the rat developing cerebral cortex. *Mol Brain Res* 103:36–48

Sun W, Funakoshi H, Nakamura T (2002*b*) Overexpression of HGF retards disease progression and prolongs life span in a transgenic mouse model of ALS. *J Neurosci* 22:6537–48

Trono D (2000) Lentiviral vectors: turning a deadly foe into a therapeutic agent. *Gene Therapy* 7:20–3

Tsuzuki N, Miyazawa T, Matsumoto K, Nakamura T, Shima K, Chigasaki H (2000) Hepatocyte growth factor reduces infarct volume after transient focal cerebral ischemia in rats. *Acta Neurochir Suppl* 76:311–6

Watanabe T, Okuda Y, Nonoguchi N, Zhao MZ, Kajimoto Y, Furutama D *et al* (2004) Post-ischemic intraventricular administration of FGF-2 expressing adenoviral vectors improves outcome and reduces infarct volume after transient focal cerebral ischemia in rats. *J Cerebr Blood Flow Metab* 24:1205–13

Williams LR, Varon S, Peterson GM, Wictorin K, Fischer W, Bjorklund A *et al* (1986) Continuous infusion of nerve growth factor prevents basal forebrain neuronal death after fimbria fornix transaction. *Proc Natl Acad Sci USA* 83:9231–5

Woodbury D, Schwarz EJ, Prockop DJ, Black IB (2000) Adult rat and human bone marrow stromal cells differentiate into neurons. *J Neurosci Res* 61:364–70

Journal of Neurochemistry, 2005, **95**, 1277–1286 doi:10.1111/j.1471-4159.2005.03446.x

Inhibition of apoptosis-inducing factor translocation is involved in protective effects of hepatocyte growth factor against excitotoxic cell death in cultured hippocampal neurons

Naoko Ishihara, Norio Takagi, Makiko Niimura, Keiko Takagi, Midori Nakano, Kouichi Tanonaka, Hiroshi Funakoshi,* Kunio Matsumoto,* Toshikazu Nakamura* and Satoshi Takeo

Department of Molecular and Cellular Pharmacology, Tokyo University of Pharmacy and Life Science, Hachioji, Tokyo, Japan
**Division of Molecular Regenerative Medicine, Course of Advanced Medicine, Osaka University Graduate School of Medicine, Suita, Osaka, Japan*

Abstract

Although hepatocyte growth factor (HGF) and its receptor are expressed in various regions of the brain, their effects and mechanism of action under pathological conditions remain to be determined. Over-activation of the *N*-methyl-D-aspartate (NMDA) receptor, an ionotropic glutamate receptor, has been implicated in a variety of neurological and neurodegenerative disorders. We investigated the effects of HGF on the NMDA-induced cell death in cultured hippocampal neurons and sought to explore their mechanisms. NMDA-induced cell death and increase in the number of terminal deoxynucleotidyl transferase-mediated dUTP-biotin nick end labeling (TUNEL)-positive cells were prevented by HGF treatment. Although neither the total amounts nor the mitochondrial localization of Bax, Bcl-2 and Bcl-xL were affected, caspase 3 activity was increased after NMDA exposure. Treatment with HGF partially prevented this NMDA-induced activation of caspase 3. Although the amount of apoptosis-inducing factor (AIF) was not altered, translocation of AIF into the nucleus was detected after NMDA exposure. This NMDA-induced AIF translocation was reduced by treatment with HGF. In addition, increased poly(ADP-ribose) polymer formation after NMDA exposure was attenuated by treatment with HGF. These results suggest that the protective effects of HGF against NMDA-induced neurotoxicity are mediated via the partial prevention of caspase 3 activity and the inhibition of AIF translocation to the nucleus.

Keywords: apoptosis-inducing factor, hepatocyte growth factor, neuronal cell death, *N*-methyl-D-aspartate receptor.
J. Neurochem. (2005) **95**, 1277–1286.

The hepatocyte growth factor (HGF), which was found to be a potent mitogen for hepatocytes (Nakamura *et al.* 1984, 1989), exerts its physiological activities as an organotrophic factor for regeneration and has protective effects in various organs (Zarnegar and Michalopoulos 1995; Matsumoto and Nakamura 1996; Balkovetz and Lipschutz 1999; Matsumoto and Nakamura 2001). In addition, motogenic, morphogenic, angiogenic and anti-apoptotic activities of HGF have been demonstrated in various types of cells (Nakamura *et al.* 1989; Zarnegar and Michalopoulos 1995; Matsumoto and Nakamura 1996; Thompson *et al.* 2004). These multipotent activities are thought to be mediated by the transmembrane tyrosine kinase receptor, c-Met (Bottaro *et al.* 1991; Higuchi and Nakamura 1991). HGF and c-Met receptor were found to be expressed in various regions of the brain and to function in a variety of ways in the central nervous system (Honda *et al.* 1995; Achim *et al.* 1997; Sun *et al.* 2002a,b). For example, HGF promoted the survival of tyrosine hydroxylase-positive midbrain neurons, as well as hippocampal and cortical neurons, during aging in culture (Honda *et al.* 1995; Hamanoue *et al.* 1996; Machide *et al.* 1998). HGF not only increased the number of calbindin D-expressing neurons in

Received May 9, 2005; revised manuscript received June 20, 2005; accepted July 18, 2005.

Address correspondence and reprint requests to Dr Norio Takagi, Faculty of Pharmaceutical Sciences, Department of Molecular and Cellular Pharmacology, Tokyo University of Pharmacy & Life Science, 1432–1 Horinouchi, Hachioji, Tokyo 192–0392, Japan.
E-mail: takagino@ps.toyaku.ac.jp

Abbreviations used: AIF, apoptosis-inducing factor; DIV, days *in vitro*; hrHGF, human recombinant hepatocyte growth factor; NMDA, *N*-methyl-D-aspartate; PFA, paraformaldehyde; PI, propidium iodide; TUNEL, terminal deoxynucleotidyl transferase-mediated dUTP-biotin nick end labeling.

postnatal rat hippocampal cultures (Korhonen *et al.* 2000), but also promoted dendritic growth and branching of layer 2 pyramidal neurons in cortical organotypic slice cultures from early postnatal mice (Gutierrez *et al.* 2004). In addition, the administration of human recombinant HGF (hrHGF) prevented neuronal death in the hippocampal CA1 region after transient global ischemia, and reduced the infarct size after transient focal cerebral ischemia and widespread cerebral embolism (Miyazawa *et al.* 1998; Tsuzuki *et al.* 2001; Date *et al.* 2004), thus suggesting that HGF has the ability to prevent ischemic brain injuries. Whereas it is conceivable that the angiogenic effect of HGF, at least in part, is involved in the rescue of the brain tissue in the *in vivo* ischemic brain, the questions remain as to whether HGF exerts protective effects by acting directly on neurons under pathological conditions, and how the effects are mediated by intracellular signalings.

The ionotropic glutamate receptors are ligand-gated ion channels that mediate the majority of excitatory neurotransmission in the central nervous system. The *N*-methyl-D-aspartate (NMDA) receptor, an ionotropic glutamate receptor, is highly permeable to Ca^{2+} and Na^{+} (Dale and Roberts 1985). Although the intracellular calcium transient induced by the influx of Ca^{2+} through the NMDA receptor plays an important role in physiological activities such as learning and memory, an excessive stimulation of the NMDA receptor has been implicated in a variety of neurological and neurodegenerative disorders, including cerebral ischemia, epilepsy, Parkinson's disease, Alzheimer's disease, Huntington's chorea and amyotrophic lateral sclerosis (Dingledine *et al.* 1999). The hippocampus plays a pivotal role in neuronal function as it is associated with learning and memory function, but it is a region vulnerable to excitotoxicity. It has become an important objective to explore strategies to protect cells from NMDA-induced excitotoxicity and to determine the underlying mechanism of such protection. In the present study, to achieve further insight into the potency of HGF treatment and the mechanism of HGF-mediated neuronal protection, we examined the effect of hrHGF treatment on NMDA-induced neurotoxicity in cultured hippocampal neurons. Our findings demonstrate inhibition of NMDA-induced apoptosis-inducing factor (AIF) translocation into the nucleus as a possible mechanism for the protective effect of HGF against excitotoxicity in hippocampal neurons.

Experimental procedures

Recombinant HGF

Human recombinant HGF (hrHGF) was purified from conditioned medium of Chinese hamster ovary cells transfected with an expression vector containing human HGF cDNA as described earlier (Nakamura *et al.* 1989). The purity of the hrHGF was > 98%, as determined by sodium dodecyl sulfate–polyacrylamide gel electrophoresis (SDS–PAGE).

Primary hippocampal cultures

Primary hippocampal cell cultures were prepared from gestational day 18 fetal rats as described previously (Huettner and Baughman 1986), with slight modifications. The hippocampi were dissected out and the cells were dissociated by incubation at 37°C for 30 min in Hank's balanced salt solution containing 15 U/mL papain, 210 U/mL deoxyribonuclease I, 1 mM L-cysteine and 0.5 mM EDTA. The dispersed cells were resuspended in Dulbecco's modified Eagle's medium containing 10% horse serum, then plated at a density of 40 000 cells/cm^2 on 12-well plates or in 35 mm dishes coated with poly-L-lysine. The medium 24 h after plating was changed to serum-free neurobasal medium containing 2% B27 supplements (Gibco-BRL, Rockville, MD, USA) and 0.5 mM glutamine. Cytosine arabinoside (1 μM) was added to inhibit the proliferation of non-neuronal cells. At 3 and 10 days *in vitro* (DIV), one half of the medium was replaced with fresh neurobasal medium containing the 2% B27 supplements and 0.5 mM glutamine. The cells were maintained at 37°C in a 5% CO_2 incubator and used for experiments at 14–16 DIV, at which time they contained 87.3 ± 4.5% NeuN-positive neurons and 12.8 ± 0.5% glial fibrillary acidic protein-positive astrocytes.

Cell viability assay

At 14–16 DIV, cells were washed twice with 10 mM HEPES buffer (washing buffer), pH 7.4, containing 144 mM NaCl, 2 mM $CaCl_2$, 1 mM $MgCl_2$, 5 mM KCl and 10 mM D-glucose. They were then incubated for 15 min at 37°C in a 5% CO_2 incubator with the desired concentration of NMDA in 10 mM HEPES buffer (stimulating buffer), pH 7.4, containing 144 mM NaCl, 2 mM $CaCl_2$, 5 mM KCl, 10 mM D-glucose and 10 μM glycine. Next, the cells were washed twice with the washing buffer and maintained in neurobasal medium containing 2% B27 supplements and 0.5 mM glutamine. After 24 h of incubation, the cells were incubated with 2 μg/mL propidium iodide (PI) for 20 min and then fixed in 4% paraformaldehyde to determine the total number of neurons by staining with anti-NeuN or anti-microtubule-associated protein 2ab (MAP2) antibody. Fluorescent images of cells were captured on a CCD camera (DP50, Olympus, Tokyo, Japan) mounted on an Olympus BX51 microscope equipped with a mercury arc lamp. The number of PI-, NeuN- or MAP2-positive cells was counted in 10 randomly chosen areas (245 × 320 μm) of each well. Results were obtained from 10 frames in four wells in four independent experiments. hrHGF was added at the desired concentrations 1 h before the addition of NMDA. For triple staining, terminal deoxynucleotidyl transferase-mediated dUTP-biotin nick end labeling (TUNEL)-positive cells were detected using an *in situ* Apoptosis Detection Kit (MK500; Takara Bio Inc., Shiga, Japan). The cells were incubated with 2 μg/mL PI for 20 min and then stained with anti-MAP2 antibody to determine the total number of neurons. The microscopic observations were performed by an operator unaware of the study group.

Western immunoblotting

Cells were homogenized in ice-cold 0.32 M sucrose containing 0.2 mM sodium orthovanadate, 0.1 mM phenylmethylsulfonyl fluoride (PMSF), and 5 μg/mL each of antipain, aprotinin and leupeptin. Some cells were homogenized and their nuclei pelleted at 1 200 *g* for 10 min. The supernatant fluid was centrifuged at 10 000 *g* for 10 min to pellet the mitochondrial fraction. Samples were stored at −80°C until used and were thawed only once. Proteins that had been

solubilized by heating at 100°C for 5 min in SDS sample buffer (10% glycerol, 5% β-mercaptoethanol and 2% SDS, in 62.5 mM Tris-HCl, pH 6.8) were separated on 8.5, 10 or 15% polyacrylamide gels and transferred to a polyvinylidene difluoride membrane. Protein blots were incubated with the appropriate antibodies, and the bound antibody was detected by the enhanced chemiluminescence method (Amersham Biosciences Inc., Piscataway, NJ, USA). Immunoblots were scanned and quantified using computerized densitometry and an image analyzer (ATTO Co., Tokyo, Japan). Care was taken to ensure that bands to be semi-quantified were in the linear range of response. For removal of bound antibodies, the blots were incubated for 30 min at 65°C in 62.5 mM Tris-HCl buffer, pH 6.8, containing 2% SDS and 0.1 M β-mercaptoethanol. The efficiency of the stripping procedure was confirmed by reacting the stripped blot with secondary antibody alone to ensure that there were no bound antibodies. Antibodies used for immunoblotting were anti-cleaved caspase 3 (Cell Signaling Technology, Inc., Beverly, MA, USA), anti-c-Met, anti-Bax, anti-Bcl-x_L (Santa Cruz Biotechnology, Inc., Santa Cruz, CA, USA), anti-Bcl-2 (BD Transduction Laboratories, San Jose, CA, USA), anti-cytochrome *c* oxidase subunit IV (Molecular Probes, Inc., Eugene, OR, USA), anti-apoptosis-inducing factor (Chemicon, Temecula, CA, USA), anti-poly(ADP-ribose) (Biomol, Plymouth Meeting, PA, USA) and anti-phosphotyrosine (clone 4G10; Upstate Biotechnology, Inc., Lake Placid, NY, USA).

Immunoprecipitation

For immunoprecipitation of c-Met, cells were lysed in 10 mM Tris-HCl buffer, pH 7.5, containing 1% Triton X-100, 150 mM NaCl, 2 mM sodium orthovanadate, 0.1 mM PMSF, and 5 μg/mL each of antipain, aprotinin and leupeptin. The lysates were pre-incubated for 1 h with protein G-agarose beads to remove any proteins that had bound non-specifically to the protein G-agarose beads. The supernatant fluid was then incubated with anti-c-Met antibody for 2 h or overnight at 4°C. Protein G-agarose beads were added and the incubation was continued at 4°C for 2 h. The immune complexes isolated by centrifugation were washed, and the bound proteins were eluted by heating at 100°C in SDS sample buffer.

Immunohistochemistry

After having been fixed with ice-cold methanol and blocked, the cells were incubated overnight at 4°C with anti-AIF antibody, and then incubated for 1 h with Cy3-conjugated anti-rabbit IgG antibody at room temperature (25 ± 2°C). Thereafter, they were incubated with anti-NeuN antibody for 2 h and then with fluorescein isothiocyanate-conjugated anti-mouse IgG antibody for 1 h. Fluorescent images of cells were captured on a CCD camera (DP50) mounted on an Olympus BX51 microscope equipped with a mercury arc lamp.

Statistics

The results were expressed as the means ± SE. Statistical comparison among multiple groups was evaluated by ANOVA followed by Fisher's protected least significant difference test.

Results

First, we confirmed the presence of the HGF receptor c-Met protein in cultured hippocampal neurons. In agreement with the results obtained from studies using cultured cortical (Machide *et al.* 1998) and cerebellar granule (Hossain *et al.* 2002) neurons, immunoblotting analysis showed that c-Met protein (140 kDa) was expressed in the cultured hippocampal neurons as well as in the adult hippocampal tissue (Fig. 1a). Also, by immunohistochemical analysis, we confirmed the expression of c-Met protein in dendrites of the cultured hippocampal neurons (Fig. 1b). To determine whether c-Met proteins in the cultured hippocampal neurons were activated in response to the application of hrHGF, we next examined the effect of hrHGF on the tyrosine phosphorylation of c-Met by performing immunoprecipitation with anti-c-Met antibody, followed by immunoblotting with anti-phosphotyrosine antibody. The tyrosine phosphorylation of c-Met was elevated relative to the initial amount as early as 10 min after the addition of 30 ng/mL hrHGF (Fig. 1c) and this increase was maintained for at least 60 min, although the amount of phosphorylated c-Met decreased gradually (Fig. 1c).

Next, hippocampal neurons were exposed to various concentrations of NMDA (10–300 μM) for 15 min. After

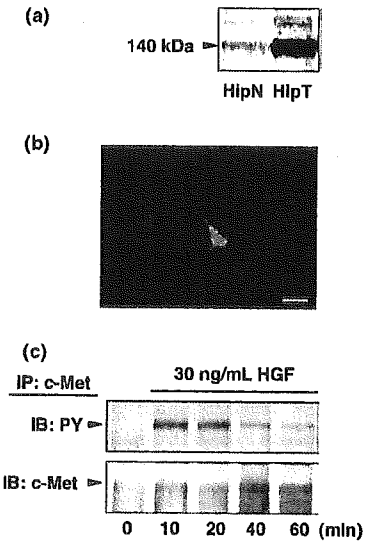

Fig. 1 Effects of hrHGF on tyrosine phosphorylation of c-Met in cultured hippocampal neurons. (a) Proteins (50 μg) from cultured hippocampal neurons at 14 DIV (HipN) and hippocampal tissue from an adult rat (HipT) were analyzed by immunoblotting with anti-c-Met antibody. c-Met protein migrated upon electrophoresis with an apparent molecular mass of 140 kDa. (b) Hippocampal neurons were fixed at 14 DIV and immunostained with anti-c-Met antibody. Scale bar represents 10 μm. (c) Proteins (200 μg) from cultured hippocampal neurons at 0, 10, 20, 40 and 60 min after treatment with 30 ng/mL hrHGF were immunoprecipitated (IP) with anti-c-Met antibody, and the precipitates were then analyzed by immunoblotting (IB) with anti-phosphotyrosine antibody (PY). The blots were then stripped and re-probed with antibody against c-Met.

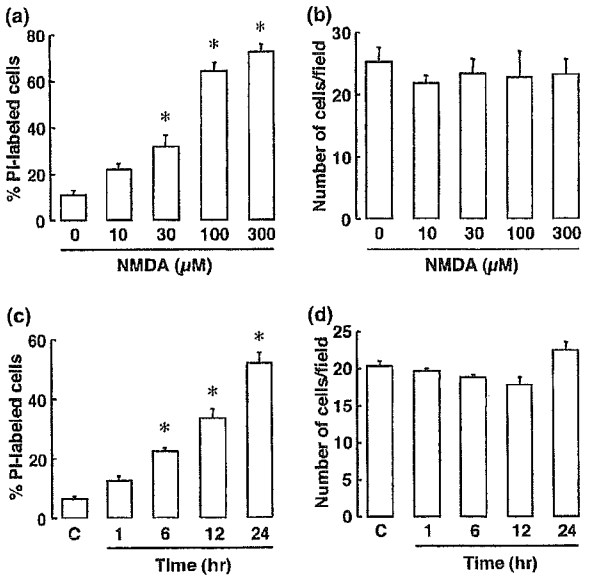

Fig. 2 Concentration-dependent profile and time course of changes in NMDA-induced excitotoxic damage in cultured hippocampal cells. (a) Cultured hippocampal cells were exposed to 10, 100 or 300 μM NMDA for 15 min. After 24 h of incubation, the cells were double-stained with propidium iodide (PI) for injured cells and anti-NeuN antibody for total neurons. *Indicates a significant difference from the NMDA-untreated group ($p < 0.05$). (b) Total number of NeuN-positive neurons counted for each condition in (a) in randomly chosen areas (245 × 320 μm). (c) Time course of the change in the number of PI-labeled cells. The percentage of PI-labeled cells among the total number of cells within the same field was determined. C indicates incubation under normal culture conditions for 24 h without pre-treatment with NMDA. *Indicates a significant difference from the NMDA-untreated group ($p < 0.05$). (d) Total number of NeuN-positive neurons counted for each condition in (c) in randomly chosen areas (245 × 320 μm). Results are the means ± SE from 10 frames in four wells in four independent experiments.

24 h of incubation under normal culture conditions, the number of PI-labeled neurons was increased (Fig. 2a) without changing the total number of neurons (Fig. 2b). The average percentages of PI-labeled cells among the total neurons (NeuN-labeled cells) treated with 0, 10, 30, 100 and 300 μM NMDA were 10.7 ± 2.2, 21.7 ± 2.6, 31.6 ± 4.9, 64.0 ± 3.7 and 72.3 ± 3.2%, respectively (Fig. 2a), and these increases were significant at the concentrations of 30, 100 and 300 μM NMDA (Fig. 2a). We next examined the time course of changes in the number of PI-labeled cells after the application of 100 μM NMDA for 15 min. The application of NMDA time-dependently increased the number of PI-labeled cells (Fig. 2c) without changing the total number of neurons (Fig. 2d). The average percentages of PI-labeled cells among the total NeuN-labeled neurons at 1, 6, 12 and 24 h after the incubation under normal conditions were 12.3 ± 1.5, 22.2 ± 1.2, 33.4 ± 3.1 and 51.9 ± 3.5%, respectively (Fig. 2c). The increase was significant from 6 h after the application of NMDA (Fig. 2c).

To determine the effects of hrHGF on NMDA-induced neuronal cell death, we added various concentrations of hrHGF to the medium containing hippocampal neurons. Treatment with hrHGF dose-dependently attenuated the increase in the number of PI-labeled cells, with the decrease being significant at 10 ng/mL hrHGF and above (Figs 3a and b). The total number of neurons counted for each condition was not changed (Fig. 3c). To further elucidate the protective effects of hrHGF against this neuronal cell death, we next investigated DNA fragmentation by TUNEL staining. The application of NMDA significantly increased the percentages of TUNEL-positive and TUNEL-PI-positive neurons (Figs 3d and e) without changing the number of neurons (Fig. 3f). Treatment with hrHGF attenuated the increase in the number of TUNEL-positive and TUNEL-PI-positive neurons (Figs 3d and e). We next examined the amounts of pro-apoptotic protein, Bax, and anti-apoptotic proteins, Bcl-2 and Bcl-xL. Not only the total amounts, but also the mitochondrial localization, of Bax, Bcl-2 and Bcl-xL, which were normalized with respect to actin or COX IV, were unaffected by the application of NMDA (Figs 4a and b). Total amounts of these proteins after the application of NMDA with hrHGF treatment were comparable with those of the non-treated control group (Fig. 4c). The effects of hrHGF on the activation of caspase 3 after the application of NMDA for 15 min were then examined. Activation of caspase 3 was assessed by immunoblotting with an antibody that recognizes the activated form of caspase 3. The application of NMDA time-dependently increased the amount of activated caspase 3 (Figs 5a and b). The average level of activated caspase 3 at 1, 12 and 24 h after incubation under normal conditions was 136.0 ± 17.0, 180.2 ± 12.8 and 221.2 ± 20.7%, respectively, of the level of the non-treated control group (Fig. 5b). The increase in activation was significant from 12 h after the incubation under normal culture conditions (Figs 5a and b). Treatment with hrHGF partially attenuated the increase in amount of activated caspase 3 at 24 h after incubation under normal culture conditions (Figs 5a and b). The average percentage of activated caspase 3 level at 24 h after incubation under normal culture conditions with hrHGF treatment was 170.6 ± 14.7% (Fig. 5b).

We next focused on caspase-independent pathways. To assess these, we determined the time course of change in the amount of AIF after the application of NMDA. The amount of AIF was not affected by NMDA application (Figs 6a and b). The intracellular localization of AIF was then investigated using double immunofluorescence histochemistry for it and the neural nuclear marker, NeuN. AIF was localized in the cytosol in control hippocampal neurons (Fig. 6c). After the application of NMDA, AIF was translocated to the nucleus at 12 (not shown) and 24 h (Fig. 6c). The application of NMDA significantly increased the percentages of AIF-

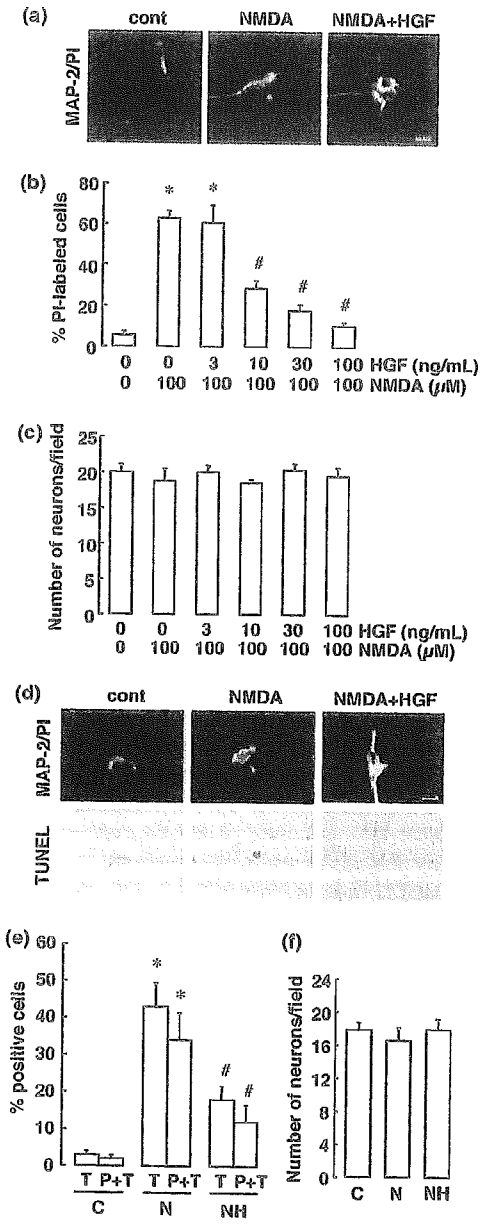

Fig. 3 Effects of hrHGF on NMDA-induced increase in the number of PI-labeled, TUNEL-positive and PI-stained/TUNEL-positive hippocampal cells. (a) Representative photomicrographs of hippocampal cells double-stained with PI (red) for injured cells and MAP2 (green) as a marker of neurons in cultures of non-treated control cells (cont) and 100 μM NMDA-treated cells without (NMDA) or with (NMDA + HGF) 30 ng/mL hrHGF. Scale bar represents 10 μm. (b) hrHGF was added at the indicated concentrations (3, 10, 30 and 100 ng/mL) 1 h before the addition of NMDA. After 24 h of incubation, the cells were double-stained with propidium iodide (PI) for injured cells and anti-MAP2 antibody for total number of neurons. (c) Total number of MAP2-positive neurons counted for each condition in (b) in randomly chosen areas (245 × 320 μm). Results are the means ± SE from 10 frames in four wells in four independent experiments. (d) Representative photomicrographs of hippocampal cells triple-stained with PI (red) for injured cells, MAP2 (green) as a marker of neuron and TUNEL for DNA-damaged cells in cultures of non-treated control cells (cont) and 100 μM NMDA-treated cells without (NMDA) or with (NMDA + HGF) 30 ng/mL hrHGF. Scale bar represents 10 μm. (e) Changes in the number of TUNEL-positive (T) and PI-stained/TUNEL-positive (P + T) cells in cultures of non-treated control cells (C) and 100 μM NMDA-treated cells without (N) or with (NH) 30 ng/mL hrHGF. The percentage of MAP2-positive cells among the total number of cells within the same field was calculated. (f) Total number of MAP2-positive neurons counted for each condition in (e) in randomly chosen areas (245 × 320 μm). Results are the means ± SE from 10 frames in four wells in four independent experiments. *Indicates a significant difference from the NMDA- and hrHGF-untreated group ($p < 0.05$). #Indicates a significant difference from the NMDA-treated and hrHGF-untreated group ($p < 0.05$).

NeuN-positive neurons (Fig. 6d) without changing the total number of neurons counted (Fig. 6e). Treatment with hrHGF attenuated the translocation of AIF to the nucleus at 24 h after the application of NMDA (Figs 6c and d) without changing the total number of neurons (Fig. 6e). We further examined poly(ADP-ribose) polymerase activity at 24 h, which was estimated by immunoblotting analysis using an anti-poly(ADP-ribose) antibody to detect poly(ADP-ribose) polymer formation. The application of NMDA significantly increased the level of poly(ADP-ribosyl)ated proteins, which were detected as diffuse bands of several molecular weights (Figs 7a and b). Treatment with hrHGF prevented poly(ADP-ribose) polymer formation (Figs 7a and b).

Discussion

We have demonstrated that treatment with hrHGF not only dose-dependently attenuates NMDA receptor-mediated neuronal cell injury, which was determined by PI uptake, but also decreases the number of TUNEL-positive and TUNEL-PI-positive hippocampal neurons, suggesting that hrHGF protects hippocampal neurons from NMDA-induced apoptotic cell death. In a recent study using mature sympathetic neurons of the superior cervical ganglion, HGF was shown to exert an anti-apoptotic effect through phosphatidylinositol-3 kinase/Akt and ERK 1/2 signaling pathways (Thompson *et al.* 2004). In addition, it was reported that HGF prevented hypoxia/reoxygenation-induced apoptosis in murine lung endothelial cells by blocking Bax translocation to the mitochondria, the blocking being mediated by the p38 MAPK pathway, and by stabilizing Bcl-xL protein levels (Wang *et al.* 2004b). However, the intracellular signaling pathways involved in protection against neuronal injuries have not been extensively studied. We found that neither the total amount nor the mitochondrial localization of Bax

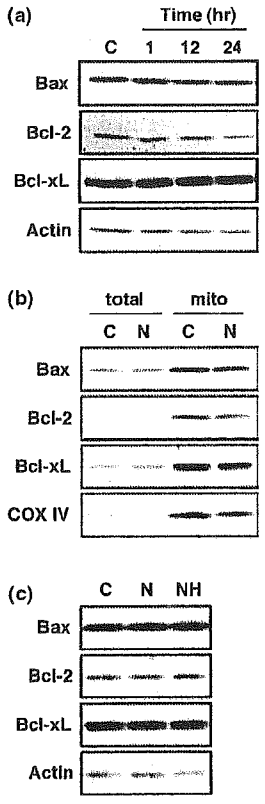

Fig. 4 Expression of apoptotic signaling proteins in cultured hippocampal neurons after the application of NMDA. (a) Cells were treated with 100 μM NMDA for 15 min, followed by incubation under normal culture conditions for 1, 12 or 24 h. Total proteins (10 μg) were analyzed by immunoblotting with anti-Bax, anti-Bcl-2, anti-Bcl-xL and anti-actin antibodies. There were no changes in the total amounts of these proteins after the application of NMDA. (b) The mitochondrial fraction was isolated 24 h after the application of NMDA, and the mitochondrial localization (mito) of Bax, Bcl-2 and Bcl-xL proteins in non-treated control (C) and 100 μM NMDA-treated (N) cells was analyzed by immunoblotting. Additional immunoblotting analysis confirmed the presence of cytochrome *c* oxidase subunit IV (COX IV) in mitochondrial fractions. (c) Effects of hrHGF on total amounts of Bax, Bcl-2 and Bcl-xL 24 h after the application of NMDA. Total proteins (10 μg) were analyzed by immunoblotting with anti-Bax, anti-Bcl-2, anti-Bcl-xL and anti-actin antibodies. Total amounts of these proteins with hrHGF treatment (NH) were comparable with those of NMDA-treated cells without hrHGF (N) and non-treated control cells (C).

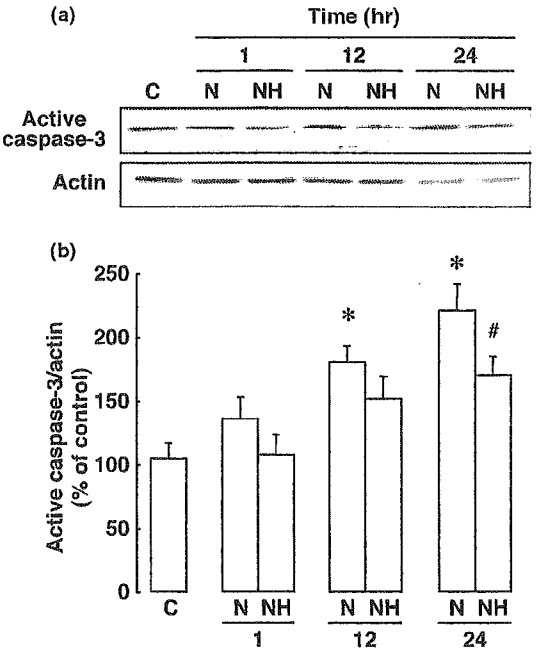

Fig. 5 Effects of hrHGF on NMDA-induced activation of caspase 3 in cultured hippocampal cells. (a) Cells were treated with 100 μM NMDA for 15 min, followed by incubation under normal culture conditions for 1, 12 and 24 h. Typical blots for cleaved caspase 3 and actin from non-treated control cells (C) and from NMDA-treated cells without (N) or with (NH) 30 ng/mL hrHGF. (b) Bands corresponding to cleaved caspase 3 and actin were scanned, and the scanned bands were normalized by actin on the same blot. Results are the means ± SE (n = 4–7). *Indicates a significant difference from the NMDA- and hrHGF-untreated group ($p < 0.05$). #Indicates a significant difference from the corresponding NMDA-treated group ($p < 0.05$).

protein was altered after the application of NMDA. The levels of Bcl-2 and Bcl-xL proteins were also unaffected, regardless of treatment with or without hrHGF. These findings suggest that the anti-apoptotic effect of HGF on hippocampal neurons was not likely to be due to the inhibition of Bax mitochondrial translocation, or increase in the expression of Bcl-2 and Bcl-xL proteins. In contrast to our findings, application of NMDA at higher concentrations, and for longer periods, to primary cultures of forebrain increased the expression of Bax relative to that of Bcl-xL (McInnis *et al.* 2002). Therefore, we cannot rule out the possibility that HGF might have the ability to protect hippocampal neurons against NMDA-induced neurotoxicity via regulation of the expression of pro- and anti-apoptotic Bcl-2 family proteins under severer pathological conditions. In this sense, it was demonstrated that HGF rapidly induced Bcl-xL expression in cardiomyocytes cultured under the condition of serum starvation (Nakamura *et al.* 2000).

Mitochondria have been shown to play a pivotal role in caspase-dependent and -independent apoptotic pathways. The caspase-dependent pathway is initiated by the release of cytochrome *c* from mitochondria, and the released cytochrome *c* associates with apoptotic protease-activating factor APAF1 to activate caspases (Danial and Korsmeyer 2004). It has been documented that the NMDA-induced apoptotic cascade consists of calcium overload of mitochondria, production of reactive oxygen species, opening of the mitochondrial permeability transition pore, release of cyto-

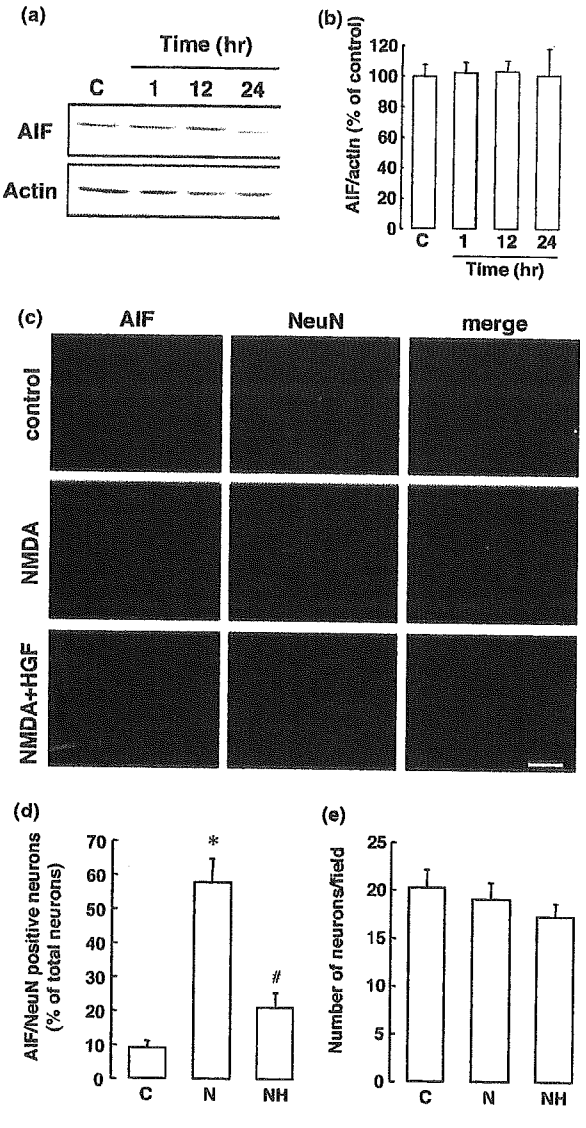

Fig. 6 Effects of hrHGF on NMDA-induced change in localization of AIF in cultured hippocampal cells. (a) Cells were treated with 100 μM NMDA for 15 min and then incubated under normal culture conditions for 1, 12 or 24 h. Total proteins (10 μg) were analyzed by immunoblotting with anti-AIF and anti-actin antibodies. (b) Bands corresponding to AIF and actin were scanned, and the scanned bands were normalized by actin on the same blot. Results are the means ± SE (n = 4–7). There were no changes in total amounts of AIF after the application of NMDA. (c) Representative photomicrographs of hippocampal cells double-stained for AIF (red) and NeuN (green), the latter being a nuclear marker of neurons in cultures of non-treated control cells (control), and 100 μM NMDA-treated cells without (NMDA) or with (NMDA + HGF) 30 ng/mL hrHGF. Scale bar represents 10 μm. (d) Changes in the number of AIF/NeuN-positive cells in cultures of non-treated control cells (C) and 100 μM NMDA-treated cells without (N) or with (NH) 30 ng/mL hrHGF. The percentage of NeuN-positive cells among the total number of cells within the same field was calculated. (e) Total number of NeuN-positive neurons counted for each condition in (d) in randomly chosen areas (245 × 320 μm). Results are the means ± SE from 10 frames in four wells in four independent experiments. *Indicates a significant difference from the NMDA- and hrHGF-untreated group ($p < 0.05$). #Indicates a significant difference from the NMDA-treated and hrHGF-untreated group ($p < 0.05$).

chrome *c* and, ultimately, activation of caspase 3 (Budd *et al.* 2000; Tenneti and Lipton 2000). In the present study, the NMDA-induced activation of caspase 3, which was comparable with the findings on cerebrocortical neurons (Budd *et al.* 2000; Tenneti and Lipton 2000; Okamoto *et al.* 2002), was partially attenuated by hrHGF treatment. Therefore, the protective effect of hrHGF, at least in part, involves inhibition of caspase-dependent pathways, although further study will be required to clarify targets of hrHGF in the caspase-dependent apoptotic cascade. It was reported that overexpression of the X chromosome-linked inhibitor of apoptosis protein, XIAP, a member of the inhibitor of apoptosis protein (IAP) family, attenuated both the activation of caspase 3 and neuronal cell death in the hippocampal CA1 region after transient forebrain ischemia (Xu *et al.* 1999). It is likely that the second baculoviral inhibitory repeat domain of XIAP is sufficient to inhibit caspases 3 and 7 (Deveraux *et al.* 1999), and that XIAP is the most potent inhibitor of caspase-dependent apoptosis (Deveraux *et al.* 1999) among the IAP family, including cIAP1, cIAP2, XIAP, NAIP, Livin/KIAP, BRUCE/Apollon and Survivin (Keane *et al.* 2001; Silke and Vaux 2001). An effective level of XIAP protein maintained by HGF might play a role in the inhibition of

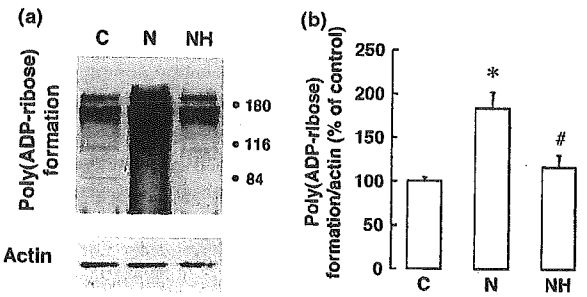

Fig. 7 Effects of hrHGF on poly(ADP-ribose) formation in cultured hippocampal cells. (a) Cells were treated with 100 μM NMDA for 15 min and then incubated under normal culture conditions for 24 h. Typical blots for poly(ADP-ribose) formation and actin from non-treated control cells (C) and 100 μM NMDA-treated cells without (N) or with (NH) 30 ng/mL hrHGF. (b) Bands corresponding to poly(ADP-ribose) formation and actin were scanned, and scanned bands were normalized by actin on the same blot. Results are the mean ± SE (n = 4–5). *Indicates a significant difference from the NMDA- and hrHGF-untreated group ($p < 0.05$). #Indicates a significant difference from the NMDA-treated and hrHGF-untreated group ($p < 0.05$).